Electronic Supplementary Information

Partially fluorinated polymer network enhances Li-ion transference number of sulfolane-based highly concentrated electrolytes

Yukako Konishi,[a] Hisashi Kokubo,[a] Seiji Tsuzuki,[b] Ryoichi Tatara [a,b] and Kaoru Dokko *[,a,b]

[a] *Department of Chemistry and Life Science, Yokohama National University, 79-5 Tokiwadai, Hodogaya-ku, Yokohama 240-8501, Japan*

[b] *Advanced Chemical Energy Research Center, Institute of Advanced Sciences, Yokohama National University, 79-5 Tokiwadai, Hodogaya-ku, Yokohama 240-8501, Japan*

*Corresponding author
E-mail address: dokko-kaoru-js@ynu.ac.jp

Experimental

Materials

Battery-grade sulfolane (SL) and lithium bis(trifluoromethanesulfonyl)amide (LiTFSA) were purchased from Kishida Chemical and used as received. 2,2,3,3-Tetrafluoropropyl methacrylate (TFPMA), 2,2,3,3,3-pentafluoropropyl methacrylate (PFPMA), diethylene glycol monomethyl ether methacrylate (DEGMA), and ethylene glycol dimethacrylate (EGDMA) were purchased from Tokyo Chemical Industry Co., Ltd. Propyl methacrylate (PMA) was obtained from Wako Pure Chemical Industries Ltd. All monomers and EGDMA were distilled under reduced pressure prior to use. 2,2′-Azobis(isobutyronitrile) (AIBN) was purchased from Wako Pure Chemical Industries Ltd. and used after recrystallization from methanol. All other reagents were purchased from Wako Pure Chemical Industries Ltd.

SL and LiTFSA were mixed at a molar ratio of [LiTFSA]/[SL] = 1:3 in an Ar-filled glovebox (dew point < −80 °C) to prepare an electrolyte solution. Gel electrolytes incorporating this electrolyte solution were also prepared in the Ar-filled glovebox. First, one of the three monomers (PMA, TFPMA, PFPMA, or DEGMA), EGDMA as a crosslinker, and AIBN as an initiator were dissolved in the electrolyte to form a homogeneous solution with a molar ratio of [LiTFSA]/[SL]/[monomer] = 1/3/n. The concentrations of the crosslinker and initiator were 2 and 1 mol% relative to the monomer, respectively. This prepolymer solution was casted into a Teflon mold, and free radical polymerization was carried out at 80 °C for 12 h to produce a gel membrane (thickness: 500 μm). We note here that phase separation was observed when PFPMA was mixed with the liquid electrolyte ([LiTFSA]/[SL] = 1:3), and a homogeneous solution was not obtained. Therefore, further experiments on the mixture of PFPMA and the liquid electrolyte were not conducted.

Characterization

Differential scanning calorimetry (DSC) measurements were performed on a NEXTA DSC200 instrument (Hitachi High-Tech Science). The samples were hermetically sealed in Al pans in an Ar-filled glovebox. The pans were heated to 100 °C to erase thermal hysteresis, cooled to −150 °C, and then re-heated to 100 °C at a heating rate of 5 °C min^{-1}. Thermograms were recorded during the final heating process.

Attenuated total reflection-Fourier transform infrared (ATR-FTIR) spectroscopy was conducted to monitor gelation using a Nicolet iS50 spectrometer (Thermo Fisher Scientific). Raman spectra of electrolytes were recorded using a Raman spectrometer (NRS-4100, JASCO) equipped with a 785 nm laser. The Raman spectrometer was calibrated using a polypropylene standard. The spectral resolution of Raman spectra was 4.5 cm^{-1}. The samples for Raman analysis were hermetically sealed in glass tubes, and their temperatures were adjusted using a Peltier microscope stage (TS62, INSTEC) with a temperature controller (mk1000, INSTEC). Pulsed-field gradient nuclear magnetic resonance (PFG-NMR) spectroscopy was conducted to evaluate the diffusivities using an ECX400 NMR spectrometer (JOEL Ltd.), with a 9.4 T narrow-bore superconducting magnet equipped with a pulsed-field gradient probe and current amplifier. The detailed experimental procedures have been reported elsewhere.[1] The samples of the gel electrolytes were prepared by the polymerization of the gel in an NMR tube (BMS-005J, Shigemi).

The ionic conductivity of the gel electrolytes was determined via the complex impedance method, using a Hewlett-Packard 4192 LF impedance analyzer at frequencies ranging from 13 MHz to 5 Hz with a sinusoidal alternating voltage amplitude of 10 mV. The ionic conductivity of the [LiTFSA]/[SL] = 1/3 electrolyte solution was measured using a conductivity cell equipped with a pair of platinized Pt electrodes. The ionic conductivity of the gel electrolyte was measured using an air-tight conductivity cell equipped with two stainless steel electrodes. The two stainless steel electrodes were separated with an O-shaped polypropylene spacer (inner diameter: 8.3 mm; thickness: 0.2 mm). The space between the two electrodes was filled with a prepolymer solution containing a monomer, EGDMA, AIBN, and a liquid electrolyte [LiTFSA]/[SL] = 1:3, and the polymerization was carried out in the air-tight conductivity cell at 80 °C for 12 h, and then, the ionic conductivity of the gel electrolyte was measured at various temperatures.

The Li-ion transference number (t_{Li+}) of the gel electrolytes was determined via a series of electrochemical impedance spectroscopy (EIS) and chronoamperometry using a Li/Li symmetric cell at 30 °C. Both the Li foil and gel membrane were punched into circular shapes (diameter: 16 mm and

thickness: 0.2 mm for Li foil; diameter: 17 mm and thickness: 0.5 mm for gel membrane). A 2032-type coin cell with a [Li/gel electrolyte/Li] configuration was assembled in an Ar-filled glovebox and left to stand overnight at 30 °C to stabilize the interface.

Electrochemical measurements of the electrolytes were performed using an electrochemical measurement system (VMP2, Biologic Science Instruments). A two-electrode cell was equipped with a Li foil (diameter: 13 mm), gel electrolyte (diameter: 13 mm; thickness: 0.5 mm), and Pt plate (diameter: 13 mm). Linear sweep voltammetry was performed to assess the oxidative stability of the electrolytes. To evaluate the reversibility of Li deposition and stripping in the electrolytes, cyclic voltammetry was conducted using a 2032-type coin cell consisting of a Li foil (diameter: 16 mm), gel electrolyte (diameter: 17 mm; thickness: 0.5 mm), and Cu foil (diameter: 16 mm). The cells were assembled in an Ar-filled glovebox, and electrochemical measurements were carried out at 30 °C.

The battery tests of the gel electrolytes were performed using a cell with a Li metal anode and porous $LiCoO_2$ composite cathode. A $LiCoO_2$ composite electrode sheet comprising $LiCoO_2$, carbon black, and poly(vinylidene fluoride) was purchased from Piotrek Co., Ltd. The mass loading of $LiCoO_2$ and thickness of the composite layer were 10.4 mg cm^{-2} and 35 μm, respectively. The areal capacity of $LiCoO_2$ on the Al foil was 1.5 mAh cm^{-2}. The $LiCoO_2$ electrode sheet was punched into circular shapes (diameter: 13.8 mm). For the charge–discharge test of a Li/$LiCoO_2$ cell with a gel electrolyte, the gelation of the electrolyte was performed in the porous $LiCoO_2$ electrode. Then, the porous $LiCoO_2$ electrode impregnated with the gel electrolyte and Li foil (diameter: 16 mm) was encapsulated in a 2032-type coin cell. Galvanostatic charge–discharge measurement of the [Li/gel electrolyte/$LiCoO_2$] cell was performed using an automatic charge–discharge instrument (Hokuto Denko HJ1010mSM8A) over the voltage range of 3.0–4.2 V at 30 °C.

DSC

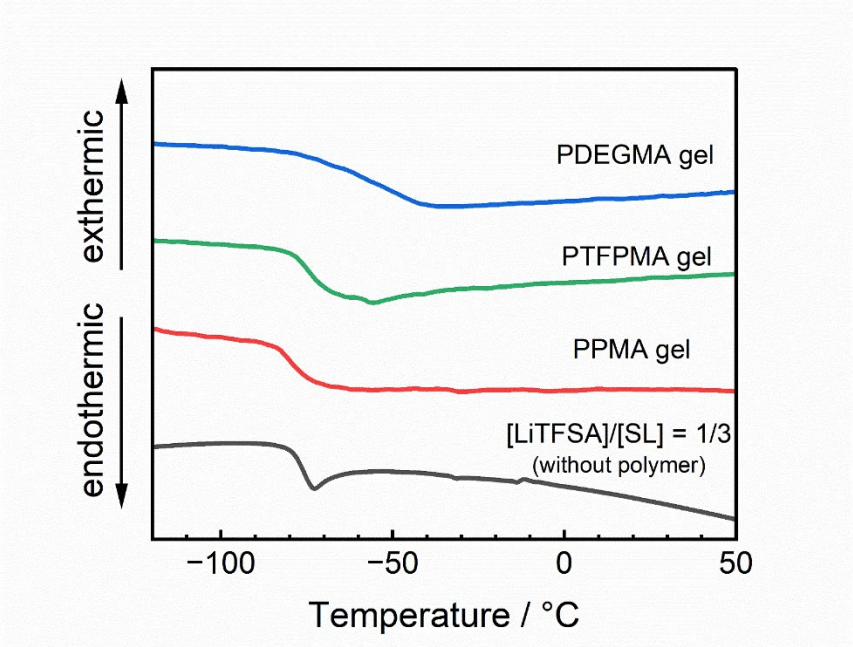

Fig. S1. DSC thermograms for the [LiTFSA]/[SL] = 1/3 solution and gel electrolytes. The composition of the gel electrolytes was [LiTFSA]/[SL]/[monomer unit] = 1/3/1.

FT-IR spectroscopy

The gelation of the electrolytes was monitored through FT-IR spectroscopy (**Fig. S1**). The disappearance of the C=C stretching vibration peak at 1640 cm^{-1} for the monomers after gelation suggested that polymerization proceeded successfully in the [LiTFSA]/[SL] = 1/3 electrolyte.

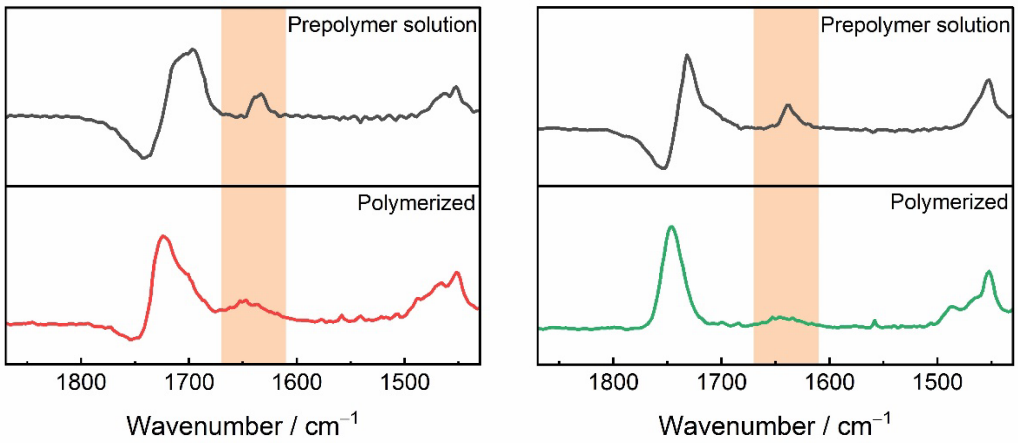

Fig. S2. FT-IR spectra of the [LiTFSA]/[SL]/[monomer unit] = 1/3/1 electrolytes before (top) and after (bottom) gelation. (a) [LiTFSA]/[SL]/[PMA] = 1/3/1 and PPMA gel electrolytes, and (b) [LiTFSA]/[SL]/[TFPMA] = 1/3/1 and PTFPMA gel electrolytes.

Raman spectroscopy

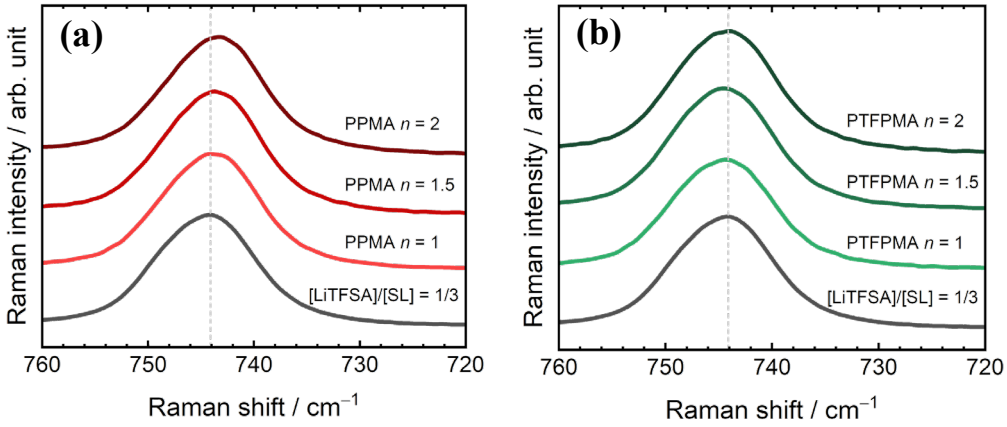

Fig. S3. Raman spectra of the [LiTFSA]/[SL] = 1/3 solution and polymer solutions [LiTFSA]/[SL]/[monomer unit] = 1/3/*n* (*n* = 1, 1.5, and 2) in the wavenumber range 720–760 cm^{-1} at 30 °C. (a) PPMA, (b) PTFPMA.

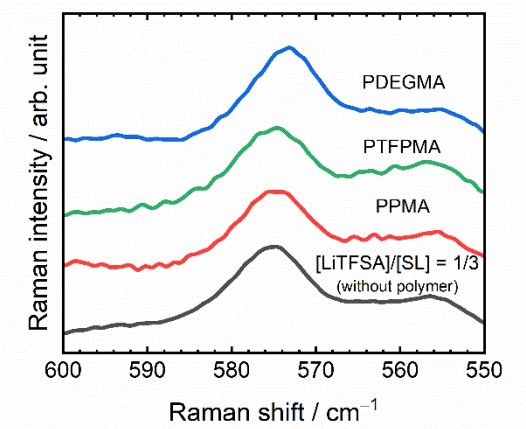

Fig. S4. Raman spectra of the [LiTFSA]/[SL] = 1/3 solution and polymer solutions [LiTFSA]/[SL]/[monomer unit] = 1/3/1 in the wavenumber range 550–600 cm^{-1}at 30 °C.

Ionic conductivity

The mass fraction of the polymer (w) in the gel electrolyte was calculated from the weight ratio of the monomer and parent electrolyte solution ([LiTFSA]/[SL] = 1/3) in the polymer precursor. The mass of LiTFSA salt in the gel electrolyte was calculated from the weight of the gel and the mass fraction of the parent electrolyte in the gel. The concentration of LiTFSA (c) in the gel was calculated from the gel volume and LiTFSA mass. The volume of the parent electrolyte in the gel was estimated from the weight of the parent electrolyte in the gel by assuming a density of the parent electrolyte (1.502 g cm^{-3}) is constant before and after the gelation. Based on this, the volume fraction of the parent electrolyte (ϕ) in the gel was estimated. These values are listed in Table S1.

Table S1. Ionic conductivity (σ), LiTFSA concentration (c), volume fraction of the parent electrolyte (ϕ), and mass fraction of the polymer (w) in the gel electrolytes [LiTFSA]/[SL]/[monomer unit] = 1/3/1 at 30 °C.

Electrolyte	σ / mS cm^{-1}	c / mol dm^{-3}	ϕ / vol%	w / wt%
[LiTFSA]/[SL] = 1/3 solution	1.04	2.32	100.0	0.0
PPMA gel	0.33	1.74	75.1	16.5
PTFPMA gel	0.23	1.70	73.1	23.6
PDEGMA gel	0.27	1.62	70.0	22.5

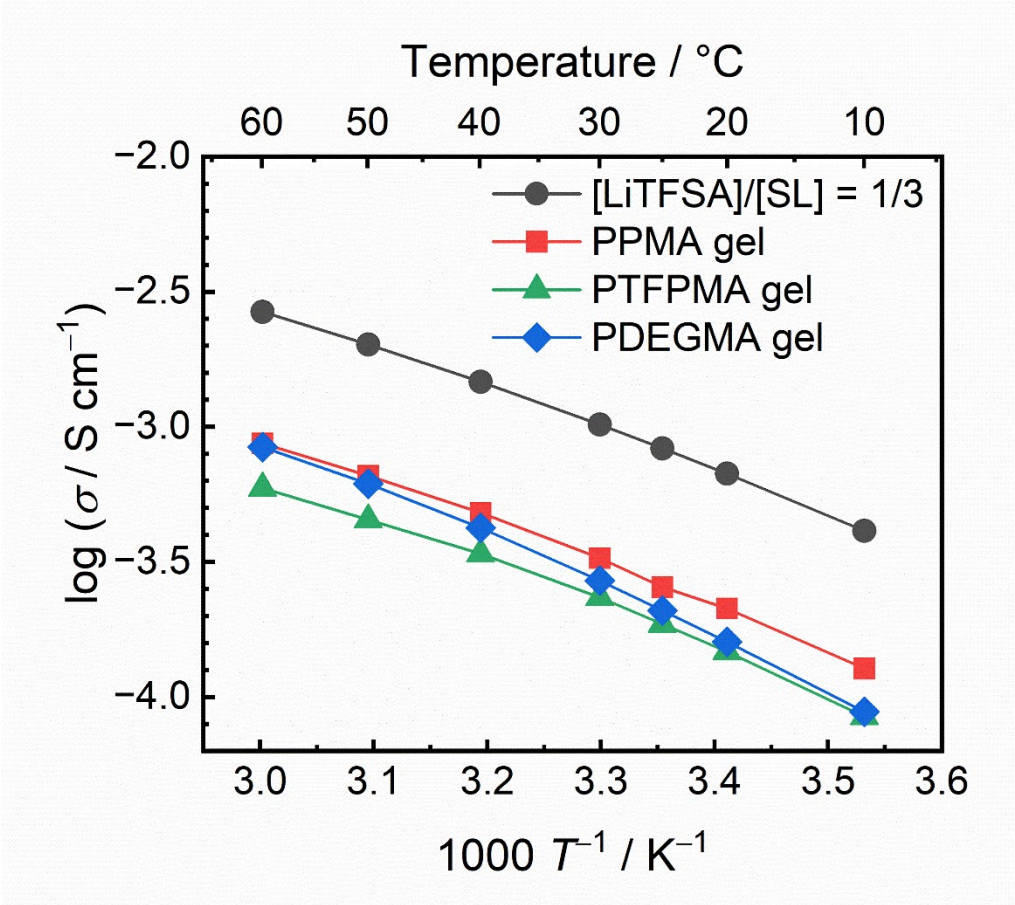

Fig. S5. Arrhenius plots for the ionic conductivity of the [LiTFSA]/[SL] = 1/3 solution and gel electrolytes. The composition of the gel electrolytes was [LiTFSA]/[SL]/[monomer unit] = 1/3/1.

Li^+ ion transference number

The Li^+ ion transference number (t_{Li+}) was estimated using a Li/Li symmetric cell under anion-blocking conditions.[2,3] A constant voltage ($\Delta V = 10$ mV) was applied to the cell for 6 h, and a chronoamperogram was recorded. EIS was performed on the same cell before and after chronoamperometry at a frequency ranging between 500 kHz and 100 mHz with a sinusoidal alternating voltage amplitude of 10 mV. t_{Li+} was calculated using the following equation.[3]

$$t_{Li+} = \frac{I_{ss}(\Delta V - I_{\Omega}R_{i,0})}{I_{\Omega}(\Delta V - I_{ss}R_{i,ss})}$$

where I_{ss} is the steady-state current in the chronoamperogram, and $R_{i,0}$ and $R_{i,ss}$ are the interfacial resistances at the Li metal electrodes determined by electrochemical measurements before and after chronoamperometry, respectively. I_{Ω} is the current calculated using Ohm's law, $I_{\Omega} = \Delta V/(R_b + R_{i,0})$, where R_b is the bulk resistance of the electrolyte in the Li/Li cell evaluated through EIS.

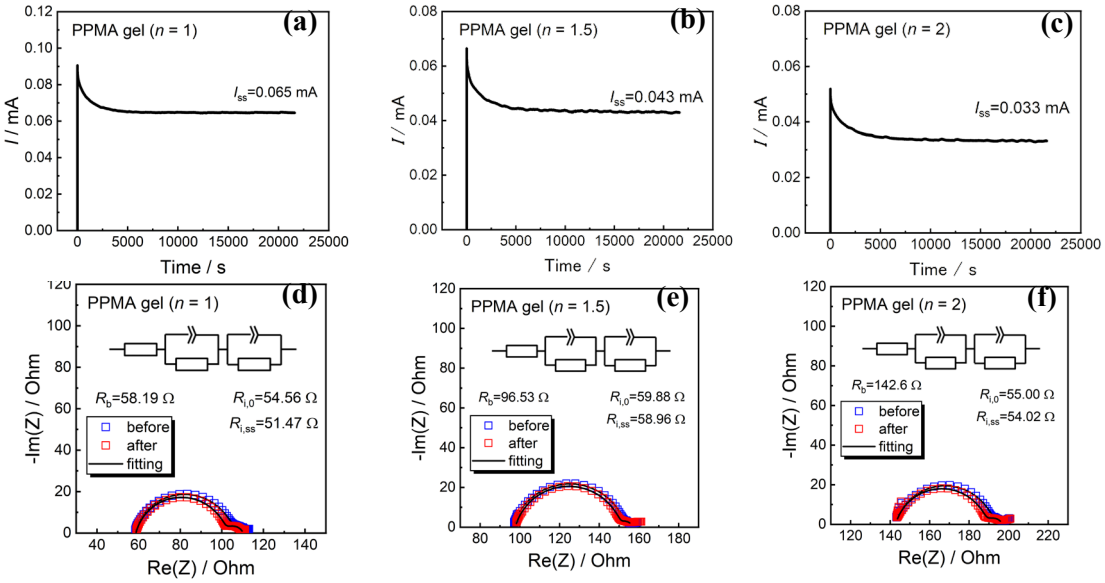

Fig. S6. (a), (b), (c) Chronoamperograms of the Li/Li symmetric cells with the PPMA gel electrolytes [LiTFSA]/[SL]/[monomer unit] = 1/3/n (n = 1, 1.5, and 2) measured at a constant voltage (ΔV) of 10 mV. (d), (e), (f) Nyquist plots of the cells before and after chronoamperometry.

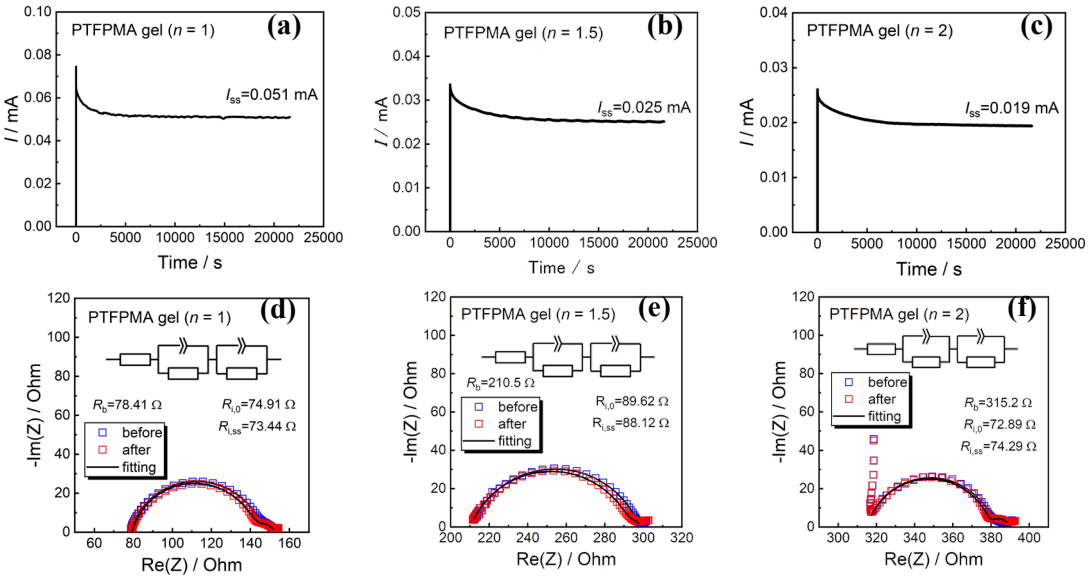

Fig. S7. (a), (b), (c) Chronoamperograms of the Li/Li symmetric cells with the PTFPMA gel electrolytes [LiTFSA]/[SL]/[monomer unit] = 1/3/n (n = 1, 1.5, and 2) measured at constant ΔV of 10 mV. (d), (e), (f) Nyquist plots of the cells before and after chronoamperometry.

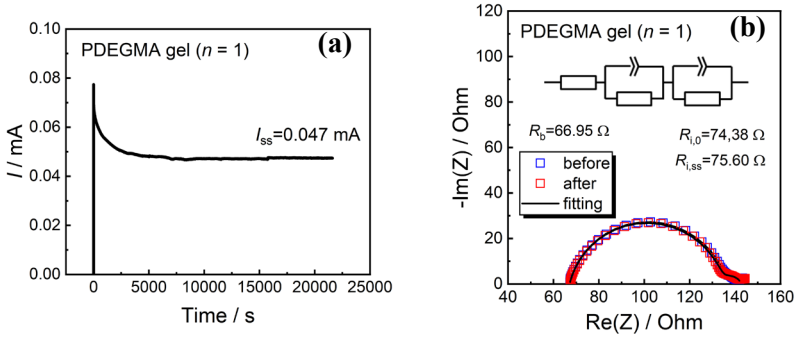

Fig. S8. (a) Chronoamperogram of the Li/Li symmetric cell with the PDEGMA gel electrolyte [LiTFSA]/[SL]/[monomer unit] = 1/3/1 measured at constant ΔV of 10 mV. (b) Nyquist plots of the cell before and after chronoamperometry.

Diffusivity

Table S2. Diffusivities of Li^+ (D_{Li+}), $TFSA^-$ (D_{TFSA-}), and SL (D_{SL}) in the [LiTFSA]/[SL] = 1/3 solution, PPMA gel, and PTFPMA gel with a composition of [LiTFSA]/[SL]/[monomer unit] = 1/3/1 at 30 °C.

Electrolyte	D_{Li+}	D_{TFSA-} / 10^{-7} cm^2 s^{-1}	D_{SL}
[LiTFSA]/[SL] = 1/3	0.977	0.741	0.953
PPMA gel	0.294	0.220	0.311
PTFPMA gel	0.232	0.152	0.230

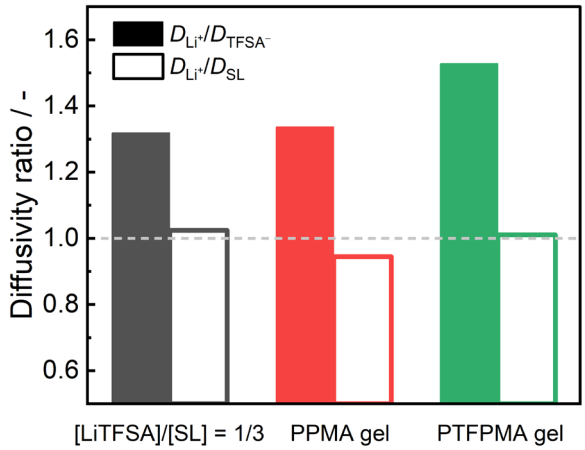

Fig. S9. Diffusivity ratios of D_{Li+}/D_{TFSA-} and D_{Li+}/D_{SL} in the [LiTFSA]/[SL] = 1/3 solution, PPMA gel, and PTFPMA gel at 30 °C. The composition of the gel electrolytes was [LiTFSA]/[SL]/[monomer unit] = 1/3/1.

Computational methods

The Gaussian 16 program [4] was used for DFT calculations. GaussView 6.1 [5] was used for visualization. The DFT calculations were carried out at the B3LYP/6-311G** level [6] with Grimme's D3 dispersion correction [7]. Optimized structures of isolated molecules were used for the calculations of electrostatic potential maps and intermolecular interaction energy potentials. The basis set superposition error (BSSE) was corrected for the interaction energy calculations using the counterpoise method [8]. In the calculations of the interaction energies between the TFSA anion and PMA, TFPMA or PFPMA, the C_2 symmetry axis of the *trans*-TFSA anion coincides with the terminal C-H or C-F bond of PMA, TFPMA or PFPMA. The distance between the nitrogen atom of TFSA and the hydrogen or fluorine atom of PMA, TFPMA or PFPMA was changed in the calculations. In the calculations of the interaction energies between the sulfolane and PMA, TFPMA or PFPMA, the bisector of the O-S-O angle of sulfolane coincides with the terminal C-H or C-F bond of PMA, TFPMA or PFPMA. The distance between the sulfur atom of sulfolane and the hydrogen or fluorine atom of PMA, TFPMA or PFPMA was changed in the calculations.

Electrostatic potential (ESP) map

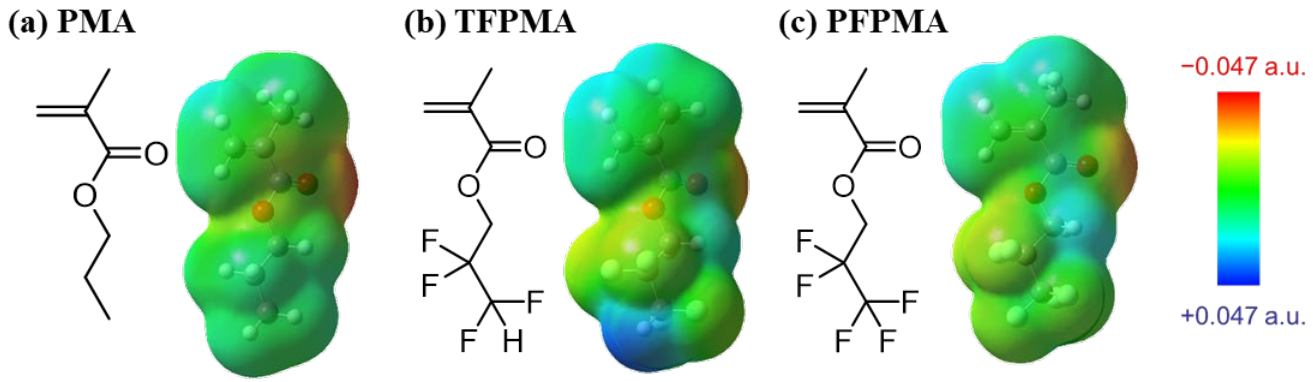

Fig. S10. Chemical structures and electrostatic potential (ESP) maps of (a) propyl methacrylate (PMA), (b) 2,2,3,3-tetrafluoropropyl methacrylate (TFPMA), and (c) 2,2,3,3,3-pentafluoropropyl methacrylate (PFPMA).

Intermolecular interaction energies

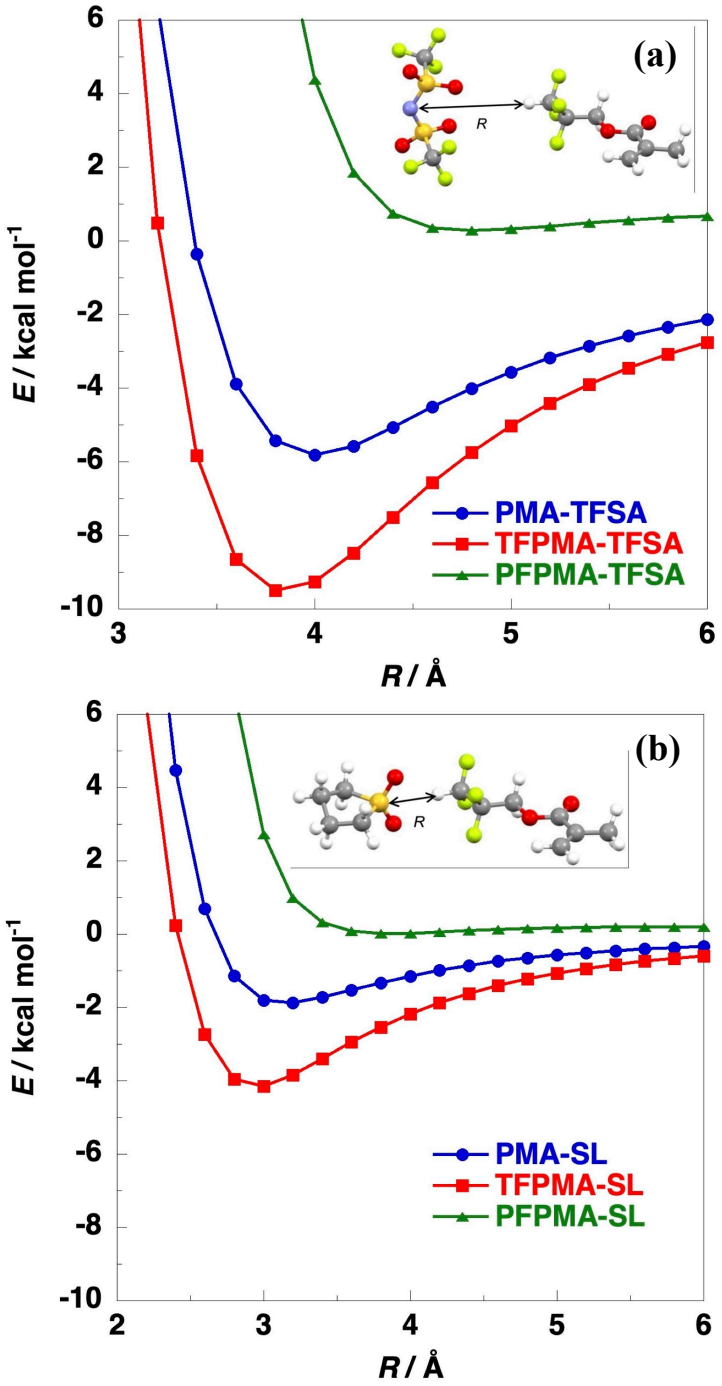

Fig. S11. (a) Intermolecular interaction energies between TFSA anion and propyl methacrylate (PMA) 2,2,3,3-tetrafluoropropyl methacrylate (TFPMA), or 2,2,3,3,3-pentafluoropropyl methacrylate (PFPMA) obtained by DFT calculations. (b) Intermolecular interaction energies between sulfolane and propyl methacrylate (PMA) 2,2,3,3-tetrafluoropropyl methacrylate (TFPMA), or 2,2,3,3,3-pentafluoropropyl methacrylate (PFPMA) obtained by DFT calculations.

Linear sweep voltammetry and cyclic voltammetry

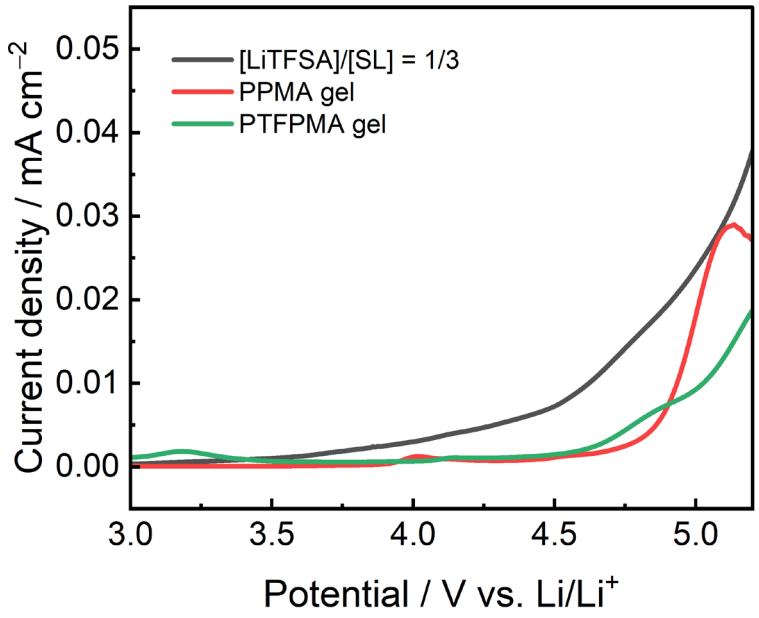

Fig. S12. Linear sweep voltammograms of the [LiTFSA]/[SL] = 1/3 solution, PPMA gel, and PTFPMA gel at a scan rate of 1 mV s^{-1} at 30 °C. The composition of the gel electrolytes was [LiTFSA]/[SL]/[monomer unit] = 1/3/1.

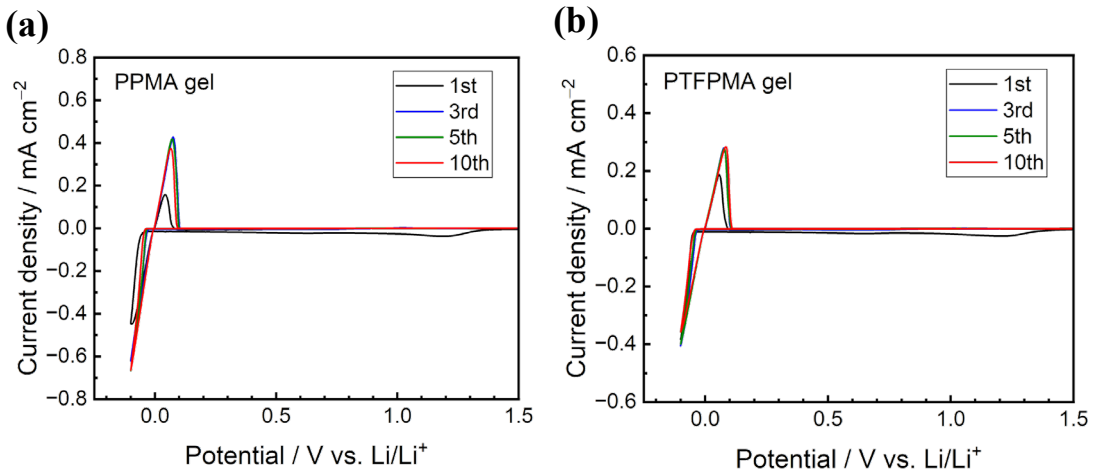

Fig. S13. Cyclic voltammograms of the (a) PPMA gel and (b) PTFPMA gel at a scan rate of 1 mV s^{-1} at 30 °C. The composition of the gel electrolytes was [LiTFSA]/[SL]/[monomer unit] = 1/3/1.

Charge–discharge test

As shown in **Fig. S11**, a porous $LiCoO_2$ electrode (diameter: 13.8 mm) was placed at the bottom of a mold. A precursor solution containing a monomer, a crosslinker (EGDMA), an initiator (AIBN), and a [LiTFSA]/[SL] = 1/3 electrolyte solution was casted into the mold and maintained at 80 °C for 12 h to form a gel electrolyte layer (thickness: 500 μm) over the $LiCoO_2$ electrode. This electrode and a Li metal electrode (diameter: 16 mm) were encapsulated in a 2032-type coin cell.

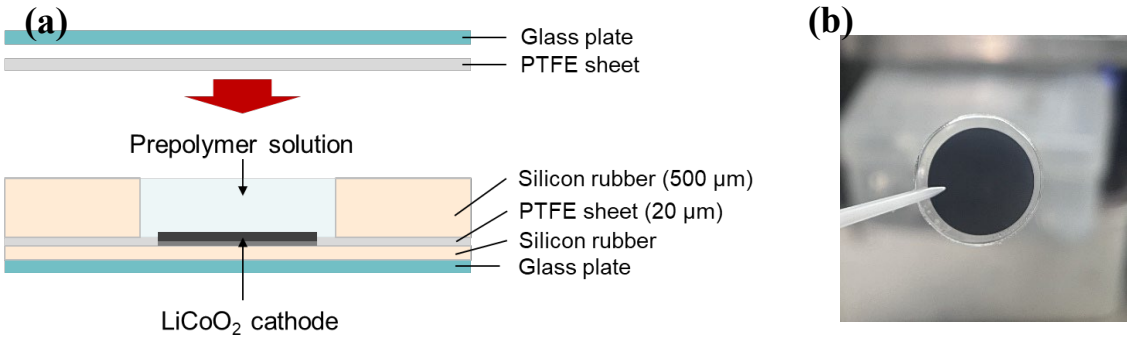

Fig. S14. (a) Schematic of the procedure to obtain a $LiCoO_2$ electrode with a 500 μm-thick gel electrolyte layer for the charge–discharge test. (b) Photograph of the $LiCoO_2$ electrode with the gel electrolyte layer.

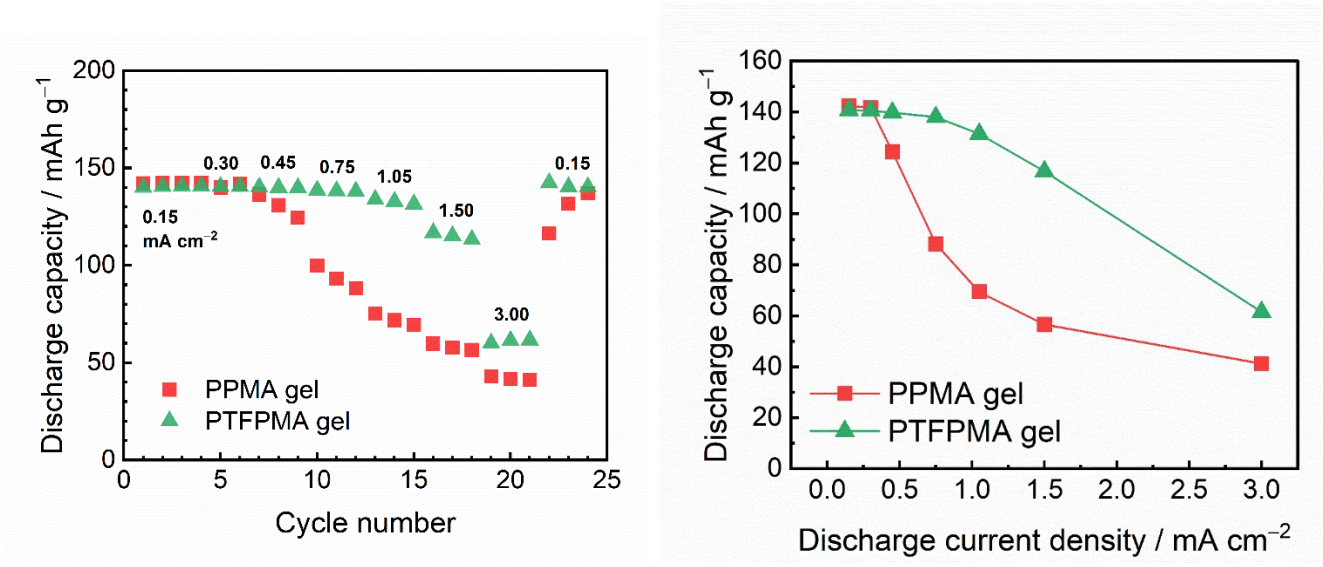

Fig. S15. Discharge capacities of the Li/$LiCoO_2$ cells with the PPMA and PTFPMA gel electrolytes measured at various discharge current densities at 30 °C. The composition of the gel electrolytes was [LiTFSA]/[SL]/[monomer unit] = 1/3/1. Prior to each discharge, the cells were charged up to 4.2 V at a low current density of 0.15 mA cm^{-2}.

References for Supplementary Information

1. Y. Ugata, M. L. Thomas, T. Mandai, K. Ueno, K. Dokko and M. Watanabe, *Phys. Chem. Chem. Phys.*, 2019, **21**, 9759–9768.
2. J. Evans, C. Vincent and P. Bruce, *Polymer*, 1987, **28**, 2324–2328.
3. M. Galluzzo, J. Maslyn, D. Shah and N. Balsara, *J. Chem. Phys.*, 2019, **151**, 020901.
4. Gaussian 16, Revision C.01, M. J. Frisch, G. W. Trucks, H. B. Schlegel, G. E. Scuseria, M. A. Robb, J. R. Cheeseman, G. Scalmani, V. Barone, G. A. Petersson, H. Nakatsuji, X. Li, M. Caricato, A. V. Marenich, J. Bloino, B. G. Janesko, R. Gomperts, B. Mennucci, H. P. Hratchian, J. V. Ortiz, A. F. Izmaylov, J. L. Sonnenberg, D. Williams-Young, F. Ding, F. Lipparini, F. Egidi, J. Goings, B. Peng, A. Petrone, T. Henderson, D. Ranasinghe, V. G. Zakrzewski, J. Gao, N. Rega, G. Zheng, W. Liang, M. Hada, M. Ehara, K. Toyota, R. Fukuda, J. Hasegawa, M. Ishida, T. Nakajima, Y. Honda, O. Kitao, H. Nakai, T. Vreven, K. Throssell, J. A. Montgomery, Jr., J. E. Peralta, F. Ogliaro, M. J. Bearpark, J. J. Heyd, E. N. Brothers, K. N. Kudin, V. N. Staroverov, T. A. Keith, R. Kobayashi, J. Normand, K. Raghavachari, A. P. Rendell, J. C. Burant, S. S. Iyengar, J. Tomasi, M. Cossi, J. M. Millam, M. Klene, C. Adamo, R. Cammi, J. W. Ochterski, R. L. Martin, K. Morokuma, O. Farkas, J. B. Foresman, and D. J. Fox, Gaussian, Inc., Wallingford CT, 2016.
5. GaussView, Version 6.1, Roy Dennington, Todd A. Keith, and John M. Millam, Semichem Inc., Shawnee Mission, KS, 2016.
6. A. D. Becke, Density-functional thermochemistry. III. The role of exact exchange, *J. Chem. Phys.* **98**, 5648-5652 (1993).
7. S. Grimme, J. Antony, S. Ehrlich, H. Krieg, A consistent and accurate *ab initio* parametrization of density functional dispersion correction (DFT-D) for the 94 elements H-Pu, *J. Chem. Phys*. **132**, 154104 (2010).
8. S. F. Boys, F. Bernardi, The calculation of small molecular interactions by the differences of separate total energies. Some procedures with reduced errors, *Mol. Phys.* **19***,* 553-566 (1970).